DETERMINATION OF OFFSHORE SPAR STOCHASTIC STRUCTURAL RESPONSE ACCOUNTING FOR NONLINEAR STIFFNESS AND RADIATION DAMPING EFFECTS

Rupak Ghosh and Pol D. Spanos

DETERMINATION OF OFFSHORE SPAR STOCHASTIC STRUCTURAL RESPONSE ACCOUNTING FOR NONLINEAR STIFFNESS AND RADIATION DAMPING EFFECTS

RUPAK GHOSH AND POL D. SPANOS

A study of the dynamic behavior of a combined dynamic system comprising a spar structure, a mooring line system, and top tensioned risers (TTR) by buoyancy can is presented. Not only the nonlinear restoring force of the mooring lines, the Coulomb friction at the compliant guides and the spar keel, and the hydrodynamic damping forces are considered, but also the effect of the frequency-dependent radiation damping is readily incorporated in this formulation. The dynamic model is subjected to input force and moment time histories that are compatible with a spectral representation (Jonswap spectrum) of a 100-year hurricane in the Gulf of Mexico. The response of the system is first determined by direct numerical integration of the equations of motion. In this regard, particular caution is exercised to treat properly the frequency-dependent terms which involve convolution transforms in the time domain. Next, a novel approach for determining the system responses is proposed. It is based on the technique of statistical linearization which can accommodate readily and efficiently the frequency-dependent elements of the dynamic system. This is achieved by appropriate modification of the system transfer function and by proper accounting for the system nonlinearities. The time domain analysis results are used to demonstrate the reliability of the statistical linearization solution. Further, the effect of the radiation damping, and the effect of the hydrodynamic forces are investigated.

A list of symbols can be found starting on page 1338.

1. Introduction

Proper concept selection for an oil/gas production facility from various options like spar, semisubmersible, and tension-leg platform (TLP) during the preliminary design phase of a project, is a daunting task since the particular choice affects the overall cost quite significantly. Among the various concepts, the spar structure is often chosen as a deep-water solution, particularly in the Gulf of Mexico. The spar appeal in the Gulf of Mexico is primarily due to its favorable motion performance under hurricane loads. The advantages of a spar structure are also manifested in the use of the dry tree riser systems and the speedy process of its delivery. Operational advantages not withstanding, the dynamic behavior of a spar structure is a quite complex problem as it has been established by several diverse studies [Agarwal and Jain 2003a; 2003b; Fischer et al. 2004; Koo et al. 2004a; 2004b; Liang et al. 2004; Tao et al. 2004; Low and Langley 2006]. An optimized spar design requires several dynamic analyses [Ran et al. 1996; 1997; 1999] involving a sufficient number of simulations of the expected load cases. These load cases reflect various environmental conditions and operational/functional criteria. In this context, it is also noted that

the ordinary time domain approach for the analysis of a coupled spar/risers/mooring lines system cannot incorporate conveniently a number of factors in the overall dynamic behavior.

Recognizing these limitations of the time domain analysis in capturing the system response statistics, Spanos et al. [2005] have suggested a computationally efficient approach for obtaining the spar responses based on a frequency domain representation. In this approach, the nonlinearities of a coupled system consisting of spar, top tensioned risers, and mooring lines are treated by using the concept of statistical linearization. Note that the statistical linearization method has already been established as a versatile tool for dynamic analysis of a nonlinear system via an auxiliary linear system, and is discussed in standard references such as [Spanos 1981a; 1981b; Roberts and Spanos 2001]. Further, based on this linearization concept, the studies by Spanos et al. have reported a reasonable agreement between the linearized responses and the nonlinear responses of an associated five-degree-of-freedom (5-DOF) dynamic model. However, these studies did not include the interaction of the hydrodynamic forces in the surge and pitch directions, and the effect of frequency-dependent damping terms. In this paper, the aforementioned linearization approach is extended to account for the interaction of the quadratic damping terms in the surge and pitch directions, and the effect of the frequency-dependent damping terms in the dynamic behavior. The theoretical developments are supplemented by appropriate numerical studies pertaining to a particular spar structure (Figure 1).

2. Spar model

The model considered here is a simplified 5-DOF coupled spar model (Figure 2) representing a truss spar (Figure 1) including fifteen top tensioned risers (TTR), and fifteen mooring lines. The spar consists of a cylindrical hard tank, of three heave plates, and of a soft tank at the bottom. The buoyancy can and stem are in contact with the spar at several preloaded guides in the center well, the heave plates, and the
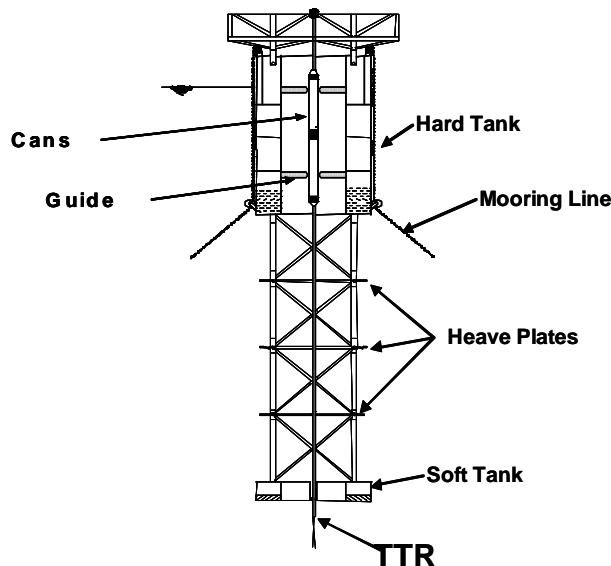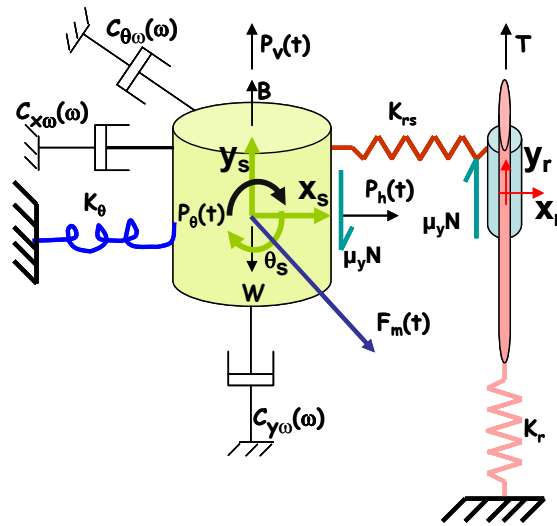

Figure 1. Typical truss spar.

Figure 2. Simplified coupled 5-DOF model.

keel. The reliability of the aforementioned simplified model in capturing the predominant features of the system dynamic behavior has been previously established by comparing its responses to specific loads to those of a full-scale detailed model [Spanos et al. 2003].

Besides the three degrees of freedom in the surge, heave and pitch directions, the riser kinematics in the surge and heave directions is also represented in the coupled model (Figure 2). In the surge direction, the mass of the spar lumped at the center of the gravity is connected to the center of gravity of the buoyancy cans/risers by a linear spring which represents a simplified account of the contact stiffness of the lateral guide. In the vertical direction, the Coulomb friction/traction force acts at the interface of the spar guide and of the buoyancy can, When sliding occurs this force depends on the relative velocity of the spar and of the buoyancy can/riser as shown in (1) and (2). Specifically, for the magnitude

$$F_f = \mu_y N, \tag{1}$$

where "N" is the force normal to the interface, and the coefficient of friction (μ_y) is represented by the equation

$$\mu_y = \mu \, \text{sgn}(\dot{y}_s - \dot{y}_r); \tag{2}$$

the symbols $\dot{y}_s$ and $\dot{y}_r$ denote the velocities in the vertical direction of the spar and of the risers/buoyancy can, respectively determining the direction of friction when sliding occurs.

The equation of motion in the surge direction (Figure 2) including both the frequency-dependent and hydrodynamic dampings is expressed by

$$M_x^s \ddot{x}_s + M_{x\theta}^s \ddot{\theta}_s + C_{sx} |\dot{x}_s + \alpha \dot{\theta}_s| (\dot{x}_s + \alpha \dot{\theta}_s) + F_{mx}(t) + K_{x\theta} \theta_s + K_{rs}(x_s - x_r) + \int_0^t C_{rx}(\tau) \dot{x}_s(t - \tau) \, d\tau$$
$$= P_h(t), \tag{3}$$

where the horizontal component of the mooring lines restoring force $F_m(t)$ is given by the equation

$$F_{mx}(t) = \alpha_1 (x_s)^3 + \alpha_2 (x_s)^2 + \alpha_3 x_s + \beta_1 y_s + C_1. \tag{4}$$

In (3), M_x^s is the mass of the spar, including the added mass in the surge direction; the symbol $K_{x\theta}$ denotes the force in the horizontal direction for unit pitch, and K_{rs} is the linear contact spring between the spar and the buoyancy can; the symbol C_{sx} is the quadratic damping coefficient; the symbols x_s, x_r and θ_s denote the spar displacement in the surge direction, the riser/buoyancy can displacement in the surge direction and the spar pitch, respectively; α introduces a factor to account for the hydrodynamic force in the horizontal direction due to the pitch motion of spar; the symbol $P_h(t)$ denotes the excitation in the surge direction; the coefficients α_1, α_2, α_3, β_1 and the constant C_1 in the polynomial in (4) have been derived by a regression analysis of the load displacement industrial data for a mooring line. Further, the coefficient C_{rx} is represented using the cosine transform of the frequency-dependent radiation damping function $\lambda_{rx}(\omega)$. That is,

$$C_{rx}(\tau) = \frac{2}{\pi} \int_0^\infty \lambda_{rx}(\omega) \cos \omega \tau \, d\omega, \tag{5}$$

Similarly, the heave motion of the spar (Figure 2) is governed by the equation

$$M_y^s \ddot{y}_s + F_{my}(t) + K_h y_s + \mu_y N + C_{sy} |\dot{y}_s| \dot{y}_s + W - B + \int_0^t C_{ry}(\tau) \dot{y}_s(t-\tau) \, d\tau = P_v(t), \tag{6}$$

where the restoring force from the mooring lines in the vertical direction is given by the equation

$$F_{my}(t) = \alpha_4 (x_s)^3 + \alpha_5 (x_s)^2 + \alpha_6 x_s + \beta_2 y_s + C_2, \tag{7}$$

with the symbol M_y^s denoting the mass of the spar including the added mass in the vertical direction. Further, K_h is the hydrodynamic stiffness of the spar in the vertical direction. The symbols W and B denote the weight and buoyancy terms of the spar. The term C_{sy} is the quadratic damping coefficient. As mentioned before the symbol N stands for the total contact preload, y_s is the heave displacement of the spar, and $P_v(t)$ is the excitation in the heave direction. The symbols α_4, α_5, α_6, and β_2 are the coefficients in the polynomial (7) and C_2 is a constant. The damping coefficient C_{ry} is represented using the cosine transform of the frequency-dependent radiation damping function $\lambda_{ry}(\omega)$. That is,

$$C_{ry}(\tau) = \frac{2}{\pi} \int_0^\infty \lambda_{ry}(\omega) \cos \omega \tau \, d\omega. \tag{8}$$

The pitch motion of the spar (Figure 2) is governed by the equation

$$J_\theta \ddot{\theta}_s^+ M_{x\theta}^s \ddot{x}_s + (T \overline{GB} + K_\theta)\theta_s + K_{x\theta} x_s + C_{s\theta} |\beta \dot{x}_s + \dot{\theta}_s|(\beta \dot{x}_s + \dot{\theta}_s) + \int_0^t C_{r\theta}(\tau)\dot{\theta}_s(t-\tau) \, d\tau = P_\theta(t), \tag{9}$$

where J_θ is the mass moment of inertia term, and K_θ is the rotational hydrodynamic stiffness. The symbol T denotes the total top tension accounting for all the risers, and $\overline{GB}$ is the distance between the center of buoyancy and the center of gravity of the spar structure. The symbol θ_s denotes the pitch of the spar, and $P_\theta(t)$ represents the excitation in the pitch direction. The symbol $C_{s\theta}$ is the quadratic damping coefficient. The damping coefficient $C_{r\theta}(\tau)$ is represented by the cosine form of the frequency-dependent radiation damping function $\lambda_{r\theta}(\omega)$. That is,

$$C_{r\theta}(\tau) = \frac{2}{\pi} \int_0^\infty \lambda_{r\theta}(\omega) \cos \omega \tau \, d\omega. \tag{10}$$

The equations of motion for the buoyancy can including the risers in the surge and heave directions (Figure 2) are

$$M_x^r \ddot{x}_r + K_{rx} x_r - K_{rs}(x_s - x_r) + \zeta_x^r 2\sqrt{K_{rx} M_x^r} \dot{x}_r = 0, \tag{11}$$

and

$$M_y^r \ddot{y}_r + K_{ry} y_r + \zeta_y^r 2\sqrt{K_{ry} M_y^r} \dot{y}_r - \mu_y N = T. \tag{12}$$

In (11) and (12), M_x^r and M_y^r are the effective mass of the risers including the buoyancy can in the horizontal and vertical directions, respectively. The symbols ζ_x^r and ζ_y^r denote the damping ratios for the risers/buoyancy can in the horizontal and the vertical directions, respectively; they are set equal to 0.05; The terms K_{rx}, and K_{ry} are the horizontal and vertical components of the riser stiffness K_r, respectively. The symbols x_r and y_r are the riser displacements in the surge and heave directions, respectively.

Note that the preceding equations of motion involve nonlinear terms, and terms represented via integral transforms. Therefore, the solution of these equations can only be obtained numerically. In this context, a standard algorithm of integrating ordinary differential equation numerically will be required. Further, the convolution integrals in equations (3), (6) and (9) must be treated by a numerical scheme.

3. Equivalent system

Alternatively to the aforementioned approach of direct numerical simulation of the equations of motion, the responses of the system can be determined by resorting to the concept of statistical linearization and pursuing a frequency domain approach.

Specifically, following [Roberts and Spanos 2001], the equivalent linear system is derived from equations (3)–(12) by replacing the nonlinear terms with equivalent linear terms. In matrix form, the equation of motion of this system can be cast in the form

$$
\begin{bmatrix}
M_x^s & 0 & M_{x\theta}^s & 0 & 0 \\
0 & M_y^s & 0 & 0 & 0 \\
M_{x\theta}^s & 0 & J_\theta & 0 & 0 \\
0 & 0 & 0 & M_x^r & 0 \\
0 & 0 & 0 & 0 & M_y^r
\end{bmatrix}
\begin{Bmatrix}
\ddot{\hat{x}}_s \\
\ddot{y}_s \\
\ddot{\theta}_s \\
\ddot{x}_r \\
\ddot{y}_r
\end{Bmatrix}
+
\begin{bmatrix}
C_{lex}+C_{x\omega} & 0 & 0 & 0 & 0 \\
0 & C_{ley}+C_{y\omega}+C_{ey} & 0 & 0 & -C_{ey} \\
0 & 0 & C_{le\theta}+C_{\theta\omega} & 0 & 0 \\
0 & 0 & 0 & C_{dx} & 0 \\
0 & -C_{ey} & 0 & 0 & C_{dy}+C_{ey}
\end{bmatrix}
\begin{Bmatrix}
\dot{\hat{x}}_s \\
\dot{y}_s \\
\dot{\theta}_s \\
\dot{x}_r \\
\dot{y}_r
\end{Bmatrix}
$$
$$
+
\begin{bmatrix}
K_{ex}+K_{rs} & 0 & K_{x\theta} & -K_{rs} & 0 \\
0 & K_{ey}+K_h & 0 & 0 & 0 \\
K_{x\theta} & 0 & T\overline{GB}+K_\theta & 0 & 0 \\
-K_{rs} & 0 & 0 & K_{rex}+K_{rs} & 0 \\
0 & 0 & 0 & 0 & K_{rey}
\end{bmatrix}
\begin{Bmatrix}
\hat{x}_s \\
y_s \\
\theta_s \\
x_r \\
y_r
\end{Bmatrix}
=
\begin{Bmatrix}
P_x(t) \\
P_y(t) \\
P_\theta(t) \\
0 \\
0
\end{Bmatrix}. \tag{13}
$$

In (13), the coefficients of the frequency-dependent radiation damping are represented by the symbols $C_{x\omega}$, $C_{y\omega}$ and $C_{\theta\omega}$ in the surge, heave and pitch directions. The effect of the static offset (x_o) representing the offset due to a steady current, is included in the analysis by introducing a time-dependent component in the system response denoted by $\hat{x}_s(t)$. That is

$$x_s = x_o + \hat{x}_s. \tag{14}$$

Further, it is required that x_s satisfies the equilibrium of (3) on the average. This leads to the equation

$$\langle \alpha_1(x_o + \hat{x}_s)^3 + \alpha_2(x_o + \hat{x}_s)^2 + \alpha_3 x_o + C_1 \rangle = P_{mh}, \tag{15}$$

with the symbol $\langle \rangle$ denoting the operator of the mathematical expectation and the symbol P_{mh} being the mean horizontal force.

Note that the linearized terms in (13) comprise an equivalent damping term to account for the energy dissipated through friction at the interface of the spar and the buoyancy can, an equivalent damping term to represent the quadratic damping, and an equivalent stiffness term to account for the nonlinearity of the mooring lines.

The spar equivalent linear stiffnesses in the horizontal and vertical directions are determined by the equations

$$K_{ex} = \left\langle \frac{\partial F_{mx}}{\partial \hat{x}_s} \right\rangle = 3\alpha_1 \sigma_{\hat{x}_s}^2 + 3\alpha_1 x_o^2 + 2\alpha_2 x_o, \tag{16}$$

and

$$K_{ey} = \left\langle \frac{\partial F_{my}}{\partial y_s} \right\rangle, \tag{17}$$

Furthermore, the linearized component of the riser stiffness in the horizontal and vertical directions are determined by the equations

$$K_{rex} = K_r \left(\frac{8}{\pi} \right)^{1/2} \frac{\sigma_{x_r} + 2x_o}{h} \tag{18}$$

and

$$K_{rey} = K_r \left(1 - \frac{0.5\sigma_{y_r}^2 + 0.5x_o^2}{h^2} \right), \tag{19}$$

where K_r represents the axial stiffness of fifteen TTRs, h represents the height of the spar center of gravity from the seabed, and $\sigma_{x_r}^2$, $\sigma_{y_r}^2$ denote the variances of the riser response in the horizontal and vertical directions, respectively.

Similarly, the nonlinear term of the friction at the compliant guide is approximated by an equivalent dashpot of value

$$C_{ey} = (\mu_y N) \left(\frac{2}{\pi} \right)^{1/2} \frac{1}{\sigma_{\dot{y}}}, \tag{20}$$

where

$$\sigma_{\dot{y}} = (\sigma_{\dot{y}_s}^2 + \sigma_{\dot{y}_r}^2)^{1/2} \tag{21}$$

with $\sigma_{\dot{y}_s}^2$ and $\sigma_{\dot{y}_r}^2$ denoting the variances of the spar and the riser/buoyancy can velocities in the vertical direction. Equations (22)–(24) refer to the quadratic damping in the surge, heave, and pitch directions. The corresponding terms in the surge, heave and pitch directions are expressed in the form

$$C_{lex} = \left(\frac{8}{\pi} \right)^{1/2} C_{sx} \left((\sigma_{\dot{x}_s})^2 + a^2 (\sigma_{\dot{\theta}_s})^2 \right)^{1/2}, \tag{22}$$

$$C_{ley} = \left(\frac{8}{\pi} \right)^{1/2} C_{sy} \sigma_{\dot{y}_s}, \tag{23}$$

$$C_{le\theta} = \left(\frac{8}{\pi} \right)^{1/2} C_{s\theta} \left(\beta^2 (\sigma_{\dot{x}_s})^2 + (\sigma_{\dot{\theta}_s})^2 \right)^{1/2}. \tag{24}$$

Obviously, the implementation of this formulation requires an iterative procedure, since the equivalent linear parameters depend on the system response, which in turn depends on the parameters. Specifically, equation (13) is recast in the form

$$M\ddot{\underline{u}} + (C + C_e)\dot{\underline{u}} + (K + K_e)\underline{u} = \underline{f}(t), \tag{25}$$

where the vector $\underline{u}(t)$ is defined as

$$\underline{u}^T = (\hat{x}_s, y_s, \theta_s, x_r, y_r) \tag{26}$$

and M, C, C_e, K and K_e represent the mass matrix, damping matrix, equivalent damping matrix, stiffness matrix, and equivalent stiffness matrix, respectively. The symbol f represents the excitation vector.

Further, the spectral matrix of the response of the equivalent system is determined from the equation

$$S_r(\omega) = H(j\omega)S_f(\omega)H'_c(j\omega), \tag{27}$$

where $S_r(\omega)$ is the power spectral density matrix of the response; $H(j\omega)$ and $H'_c(j\omega)$ are the transfer functions of responses and its complex conjugate transposed, respectively. The transfer function $H(j\omega)$ is given by the equation

$$H(\omega) = \left[-\omega^2 M + i\omega(C + C_e) + (K + K_e)\right]^{-1}. \tag{28}$$

The symbol $S_f(\omega)$ represents the power spectral density of the excitations. Note that in each iteration step, the variances of various response components are determined by using the "generic" equations

$$\sigma_r^2 = \int_{-\infty}^{\infty} S_r(\omega)\,d\omega \quad \text{and} \quad \sigma_{\dot{r}}^2 = \int_{-\infty}^{\infty} \omega^2 S_r(\omega)\,d\omega, \tag{29}$$

where σ_r^2 and $\sigma_{\dot{r}}^2$ are generic response displacement and response velocity variances, and $S_r(\omega)$ is the associated spectral density of displacement.

A set of new responses statistics is obtained based on the response from (27) and the iteration continues until convergence in the response statistics is achieved.

4. Numerical results

The preceding two approaches — numerical integration of the governing equation in the time domain and frequency domain solution based on the statistical linearization — are used to study the responses of a coupled system consisting of truss spar, mooring lines, and riser. The total weight of the truss spar is approximately 163,960 t. The radius of hull and draft are 23.8 m and 198.1 m, respectively. Each top tensioned riser is tensioned by using a buoyancy can which transfers tension to the riser at top. The diameter and the height of each buoyancy can are 3.65 m and 73 m, respectively. In this context, the comparison of the nonlinear responses with the responses from the equivalent model is presented for two different load cases. The difference in two load cases is that one of the two load cases includes the effect of the current associated with the 100-year hurricane wave whereas the other load case accounts for the effect due to the 100-year hurricane wave only. As a result of the steady current, the spar in one case will have a static offset from the neutral position. The significant wave height and peak period of the 100-year event are considered as 12.5 m and 14.0 sec. The input excitations for the simplified model

(Figure 2) analysis are specified in the form of force and moment time histories at the center of gravity of the spar. The excitations $P_h(t)$, $P_v(t)$ and $P_\theta(t)$ are obtained from a detailed model analysis [Spanos et al. 2003] by using the motion analysis program MLTSIM [Pauling 1995].

The nonlinear responses are obtained by numerically integrating the equations of motion (3)–(12), which also accounts for the effect of the frequency-dependent radiation damping specified from an industrial data set and plotted in Figure 3.

Step-by-step (0.1 sec) numerical integration is carried out by using the fourth order Runge–Kutta scheme. The linearized responses are determined from the equivalent model by iterations using equations
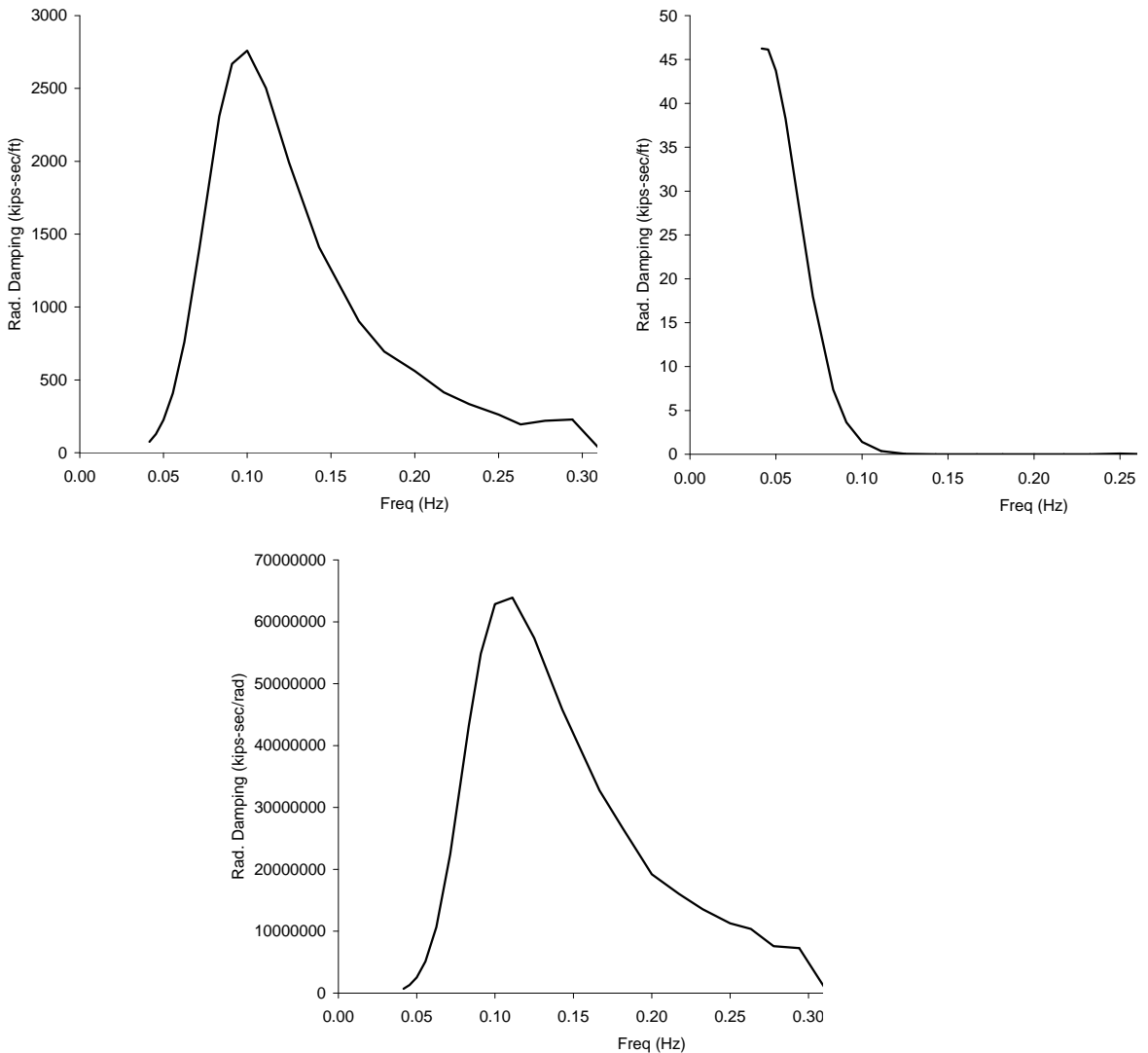

Figure 3. Frequency-dependent damping in the surge direction (top left), in the heave direction (top right), and in the pitch direction (bottom). 1 kips equals 4.447 kN and 1 kips sec/ft equals 14.59 kN sec/m.

Displacement	Wave forces only		Wave forces + Current	
	Nonlinear analysis	Stat. linearization	Nonlinear analysis	Stat. linearization
Surge (m)	1.60	1.64	1.49	1.58
Heave (m)	0.06	0.05	0.05	0.04
Pitch (rad)	0.01	0.01	0.01	0.01

Table 1. Comparison of root mean square responses: nonlinear analysis vs. statistical linearization.

(13)–(29). The root mean square responses in the surge, heave and pitch directions from both analyses are presented in Table 1. The agreement in the response statistics determined by the two approaches is quite reasonable. Clearly, response variances alone do not provide complete insight of the responses in various frequencies ranges. Hence, the power spectral densities of the linear and nonlinear responses are compared to examine the agreement of the responses in the low and wave frequency regions. Figure 4 shows comparisons of the surge, heave and pitch responses for the wave-induced forces only (that is, the effect of currents is not included). It reveals that the linearized surge response is conservative at the natural frequency and peak wave frequency which explains the higher rms surge from the equivalent
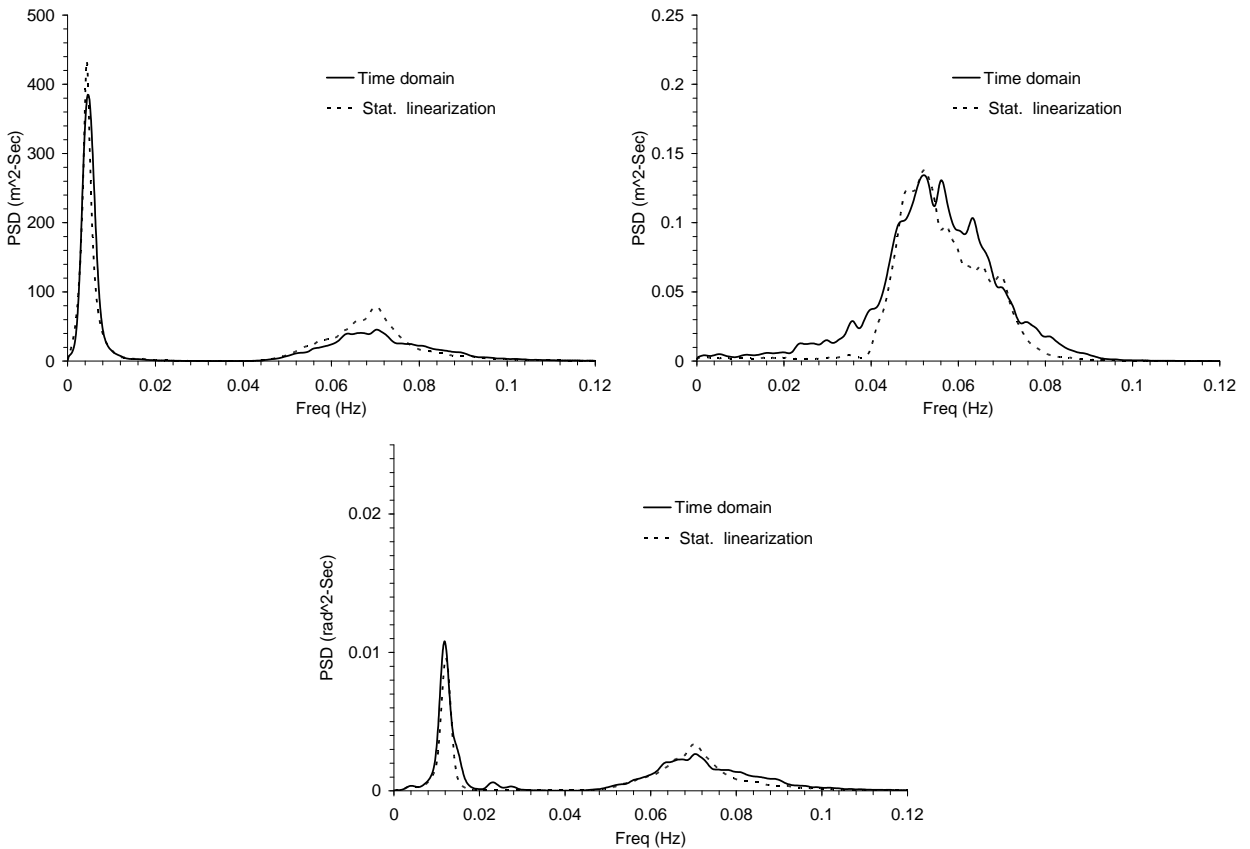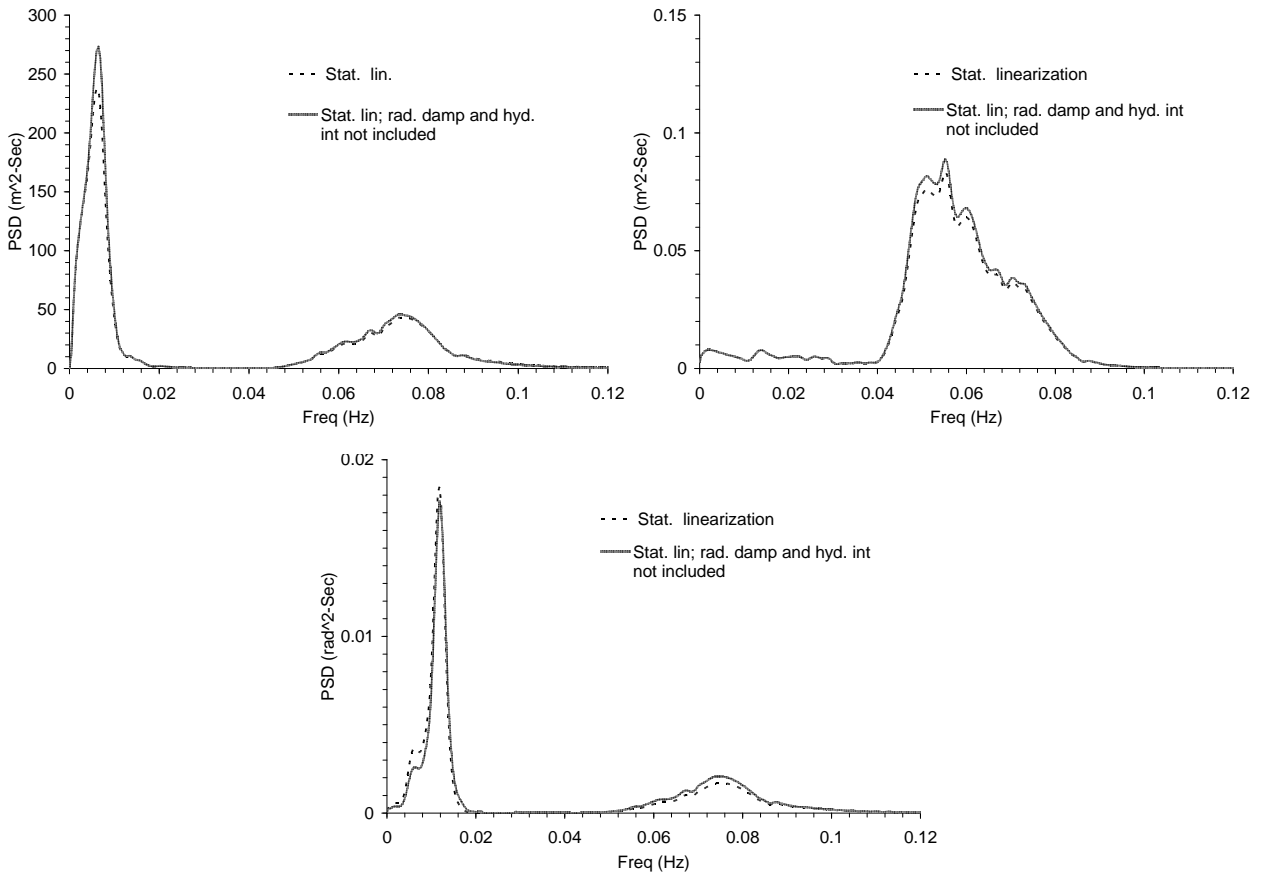

Figure 4. Comparison of the surge (top left), heave (top right) and pitch (bottom) responses for wave-induced forces only (no current).

model analysis. The linearization of Coulomb damping in the equivalent system underpredicts the heave response to an acceptable limit (Figure 4, top right). The pitch response (Figure 4, bottom) exhibits an acceptable agreement at all frequencies.

Next, a comparison of the surge, heave and pitch responses (Figure 5) for the wave-induced forces and current exhibits a trend similar to the one observed in the wave-induced case. The surge and the heave responses (top row in this figure) at the offset position are less than the surge and the heave responses (top row in Figure 4) at the mean position. This trend is persistent irrespective of the analysis methods. The natural frequency of the system in the surge direction is increased due to higher stiffness contribution by the TTRs and mooring lines at the offset position. The heave response comparison (Figure 5, top right) shows that the linearized response is under-predicted at all frequencies to a small extent, and shows similar effect of the Coulomb damping as observed in the previous case. Besides the linearized Coulomb damping, another contributing factor in the reduction of the heave response (top right panels in Figures 4 and 5) at the offset position is the increased stiffness of the mooring lines. Finally, excellent agreement of the pitch responses is obtained in the wave frequency region whereas the equivalent response is conservative in the low frequency region.
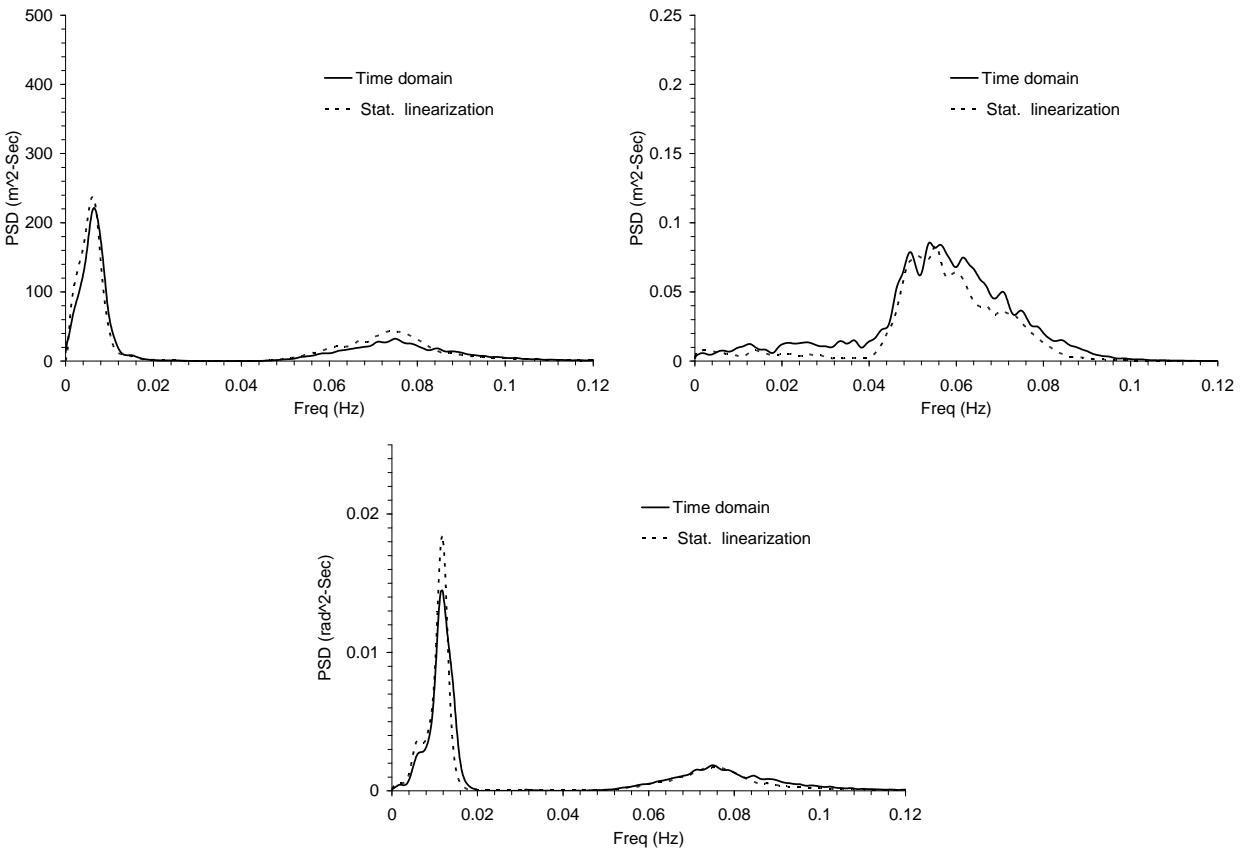
Figure 5. Comparison of the surge (top left), heave (top right) and pitch (bottom) responses for wave- and current-induced forces.

Figure 6. Comparison of the surge (top left), heave (top right) and pitch (bottom) responses, showing effect of hydrodynamic interaction and frequency-dependent damping.

The effect of hydrodynamic interaction and frequency-dependent damping is examined by comparing the linearized responses only. The responses without the effect of frequency-dependent damping and hydrodynamic interaction were earlier reported [Spanos et al. 2005] and included in this paper for comparison study only. This comparison is discussed for the load case consisting of the wave and current only. Figure 6, top left, shows the response comparison in the surge direction. It is apparent that the hydrodynamic interaction and frequency-dependent damping affects the surge response at the natural frequency only. Similarly, the effect on the heave response (Figure 6, top right) is also reflected close to the spar natural period. The spar natural period at the offset position is approximately 18.2 sec assuming the buoyancy can sticks to the hull. The effect in the pitch direction (Figure 6, bottom) is not significant.

5. Concluding remarks

A frequency domain analysis approach for a coupled spar/risers/mooring lines system has been presented. This approach has been used to study the spar dynamic behavior, as well as to assess the effect of the spar/riser/mooring lines interaction on the spar response characteristics. The approach offers the desirable

features of incorporating in the analysis various effects such as that of the nonlinearities of the mooring lines, that of the hydrodynamic damping, and that of frequency-dependent parameters associated with radiation damping. Note that frequency-dependent parameters are ordinarily accounted for in offshore structural dynamics by using elaborate convolution techniques in time domain analyses. However, these parameters have been dealt readily in the frequency domain solution approach presented herein by using the concept of transfer function. Furthermore, the transfer function, appropriately modified, has accounted readily for various nonlinearities of the spar/mooring lines/riser system by using the technique of statistical linearization.

In the studies reported herein it has been found out that the hydrodynamic interaction in the surge and pitch directions and the radiation damping affect considerably the spar responses in the surge and the heave directions; indeed the spectral values at the vicinity of natural frequencies in the surge and the heave directions have been reduced when these parameters were included. Note, however, that this conclusion relates to the particular system and sea-states considered in the present study. Obviously, a qualitatively different conclusion may be derived for other design scenarios.

Clearly a convenient assessment tool can be quite useful for sizing of spar structures as well as for the selection of the number, orientation, and kind of mooring lines (steel wire vs. polyester), in the early stage of any offshore field development. This is also true for the selection of a proper riser system with respect to a spar. This is due to the fact that the characteristics of the spar motion influence the spar-riser interface design. The design options are that of top tensioned riser supported by the buoyancy can (considered herein), and that of a steel catenary riser system; obviously even the latter design option can be readily treated by the herein proposed approach. Note that for a high pressure riser system, the interface load can be significant due to increased wall thickness and associated hull size increases to accommodate higher payloads. In this case the large spar hull size will, of course, influence the riser dynamic responses/fatigue life as well as the hull fabrication and installation cost, and will have a major impact on the total cost of a project. In this regard, a convenient approach like the one presented herein may be used as a reliable tool for a rapid assessment of the merits of the various riser/spar interface scenarios.

Index of notation

α: A factor to capture the hydrodynamic force in the surge direction due to unit pitch

$\alpha_1, \alpha_2, \alpha_3, \beta_1$: Coefficients in the polynomial giving the mooring line load-displacement relation; surge direction

$\alpha_4, \alpha_5, \alpha_6, \beta_2$: Coefficients in the polynomial giving the mooring line load-displacement relation; heave direction

B: Total buoyancy of the spar

β: A factor to capture the hydrodynamic force in the pitch direction due to unit surge

C: Linear damping matrix for the multi-degree-of-freedom system

C_1/C_2: Constant in the polynomial representing mooring line load-displacement relation; surge/heave direction

C_{dx}/C_{dy}: Damping of the risers/buoyancy can in the surge/heave direction

$C_{sx}/C_{sy}/C_{s\theta}$: Quadratic damping coefficient in the surge/heave/pitch direction

$C_{x\omega}/C_{y\omega}/C_{\theta\omega}$: Frequency-dependent radiation damping in the surge/heave/pitch direction

C_e: Equivalent damping matrix for the multi-degree-of-freedom system

$C_{lex}/C_{ley}/C_{le\theta}$: Equivalent linear damping of the spar in the surge/heave/pitch direction

C_{ey}: Equivalent Coulomb damping in the heave direction

$C_{rx}(\tau)/C_{ry}(\tau)/C_{r\theta}(\tau)$: Damping impulse function in the surge/heave/pitch direction

$\underline{f}(t)$: Force vector representing all excitations

$\overline{F}_f$: Friction force at the spar and buoyancy can contact surface

$F_m(t)$: Restoring force in the mooring lines

$F_{mx}(t)/F_{my}(t)$: Restoring force in the mooring lines in the surge/heave direction

$\overline{GB}$: Distance between center of buoyancy and center of gravity of the spar

h: Height of the center of gravity of the spar from the seabed

$H(j\omega)$ and $H'_c(j\omega)$: Frequency response function of the spar and its transpose conjugate

J_θ: Mass moment inertia in the pitch direction

K: Linear stiffness matrix for the multi-degree-of-freedom system

K_e: Equivalent stiffness matrix for the multi-degree-of-freedom system

K_{ex}/K_{ey}: Equivalent stiffness of the spar in the surge/heave direction

K_h/K_θ: Hydrodynamic stiffness of the spar in the heave/pitch direction

$K_{x\theta}$: Force in the surge direction due to unit pitch

K_{rs}: Contact stiffness of the guide between the buoyancy can and the spar

K_r: Total axial stiffness of riser system

K_{rx}/K_{ry}: Riser stiffness in the surge/heave direction

K_{rex}/K_{rey}: Equivalent riser stiffness in the surge/heave direction

$\lambda_{rx}(\omega)/\lambda_{ry}(\omega)/\lambda_{r\theta}(\omega)$: Frequency-dependent radiation damping function; surge/heave/pitch direction

M: Mass matrix for the multi-degree-of-freedom system

M_x^s, M_y^s: Mass of the spar including the added mass in the surge/heave direction

M_x^r, M_y^r: Mass of the risers/buoyancy can including the added mass in the surge/heave direction

$M_{x\theta}^s$: Coupling mass term between surge and pitch direction

μ: Coefficient of the Coulomb friction at the spar and buoyancy can contact surface

N: Total preload at the spar/buoyancy can contact guide

$P_h(t)/P_v(t)/P_\theta(t)$: Excitation in the surge/heave/pitch direction

P_{mh}: Mean force in the surge direction

$S_r(\omega)/S_f(\omega)$: Spectral density matrix of the responses/excitations

$\sigma_{x_r}^2/\sigma_{y_r}^2$: Variance of the riser response in the surge/heave direction

$\sigma_{\hat{x}_s}^2/\sigma_{\dot{y}_s}^2/\sigma_{\theta_s}^2$: Variance of the spar response in the surge/heave/pitch direction

σ_r^2: Generic response displacement variance

$\sigma_{\dot{r}}^2$: Generic response velocity variance

T: Total top tension in the risers

$\theta_s r/\dot{\theta}_s/\ddot{\theta}_s$: Spar rotation/velocity/acceleration in the pitch direction

$\underline{u}$: Displacement vector

W: Total weight of the spar

x_o: Static offset of the spar in the surge direction

x_r/y_r: Risers/buoyancy can displacement in the surge/heave direction

$\dot{x}_r/\dot{y}_r$: Risers/buoyancy can velocity in the surge/heave direction

$\ddot{x}_r/\ddot{y}_r$: Risers/buoyancy can acceleration in the surge/heave direction

x_s/y_s: Total spar displacement in the surge/heave direction

$\dot{x}_s/\dot{y}_s$: Spar velocity in the surge/heave direction

$\ddot{x}_s/\ddot{y}_s$: Spar acceleration in the surge/heave direction

$\hat{x}_s$: Time-dependent component of the surge of the spar

ζ_x^r/ζ_y^r: Damping coefficient for the risers/buoyancy can in the surge/heave direction

References

[Agarwal and Jain 2003a] A. K. Agarwal and A. K. Jain, "Dynamic behavior of offshore spar platforms under regular sea waves", *Ocean Eng.* **30**:4 (2003), 487–516.

[Agarwal and Jain 2003b] A. K. Agarwal and A. K. Jain, "Nonlinear coupled dynamic response of offshore spar platforms under regular sea waves", *Ocean Eng.* **30**:4 (2003), 517–551.

[Fischer et al. 2004] F. J. Fischer, S. I. Liapis, and Y. Kallinderis, "Mitigation of current-driven vortex-induced vibrations of a spar platform via "SMART" thrusters", *J. Offshore Mech. Arct. Eng.* **126**:1 (2004), 96–104.

[Koo et al. 2004a] B. J. Koo, M. H. Kim, and R. E. Randall, "The effect of nonlinear multi-contact coupling with gap between risers and guide frames on global spar motion analysis", *Ocean Eng.* **31**:11–12 (2004), 1469–1502.

[Koo et al. 2004b] B. J. Koo, M. H. Kim, and R. E. Randall, "Mathieu instability of a spar platform with mooring and risers", *Ocean Eng.* **31**:17–18 (2004), 2175–2208.

[Liang et al. 2004] N.-K. Liang, J.-S. Huang, and C.-F. Li, "A study of spar buoy floating breakwater", *Ocean Eng.* **31**:1 (2004), 43–60.

[Low and Langley 2006] Y. M. Low and R. S. Langley, "Time and frequency domain coupled analysis of deepwater floating production systems", *Appl. Ocean Res.* **28**:6 (2006), 371–385.

[Pauling 1995] J. R. Pauling, "MLTSIM: time domain platform simulation for floating platform consisting of multiple interconnected bodies", 1995.

[Ran and Kim 1997] Z. Ran and M. H. Kim, "Nonlinear coupled responses of a tethered spar platform in waves", *Int. J. Offshore Polar Eng.* **7**:2 (1997), 111–118.

[Ran et al. 1996] Z. Ran, M. H. Kim, J. M. Niedzwecki, and R. P. Johnson, "Responses of a spar platform in random waves and currents: experiment vs. theory", *Int. J. Offshore Polar Eng.* **6**:1 (1996), 27–34.

[Ran et al. 1999] Z. Ran, M. H. Kim, and W. Zheng, "Coupled dynamic analysis of a moored spar in random waves and currents: time-domain vs. frequency-domain analysis", *J. Offshore Mech. Arct. Eng.* **121**:3 (1999), 194–200.

[Roberts and Spanos 2001] J. B. Roberts and P. D. Spanos, *Random vibrations and statistical linearizations*, Dover, New York, 2001.

[Spanos 1981a] P. D. Spanos, "Stochastic linearization in structural dynamics", *Appl. Mech. Rev.* (*ASME*) **34**:1 (1981), 1–8.

[Spanos 1981b] P. D. Spanos, "Monte Carlo simulations of responses of non-symmetric dynamic systems to random excitations", *Comput. Struct.* **13**:1–3 (1981), 371–376.

[Spanos et al. 2003] P. D. Spanos, R. Ghosh, L. D. Finn, and J. E. Halkyard, "Coupled analysis of a spar structure: Monte Carlo and statistical linearization solutions", in *Proceedings of the 22nd International Conference of Offshore Mechanics and Arctic Engineering* (*OMAE 2003*) (Cancun, 2003), edited by S. Chakrabarti and T. Kinoshita, ASME, New York, 2003. Paper # OMAE2003-37414.

[Spanos et al. 2005] P. D. Spanos, R. Ghosh, L. D. Finn, and J. E. Halkyard, "Coupled analysis of a spar structure: Monte Carlo and statistical linearization solutions", *J. Offshore Mech. Arct. Eng.* **127**:1 (2005), 11–16.

[Tao et al. 2004] L. Tao, K. Y. Lim, and K. Thiagarajan, "Heave response of classic spar with variable geometry", *J. Offshore Mech. Arct. Eng.* **126**:1 (2004), 90–95.

RUPAK GHOSH: Rupak.Ghosh@bp.com

POL D. SPANOS: spanos@rice.edu
Rice University, Departments of Civil and Mechanical Engineering, 6100 Main Street, Mail Stop 321, Houston, TX 77005-1892, United States